Limits on achievable dimensional and photon efficiencies with intensity-modulation and photon-counting due to non-ideal photon-counter behavior

Bruce Moision, Baris I. Erkmen, William Farr, Samuel J. Dolinar, and Kevin M. Birnbaum

Jet Propulsion Laboratory, California Institute of Technology,
4800 Oak Grove Dr., Pasadena, CA 91109

ABSTRACT

An ideal intensity-modulated photon-counting channel can achieve unbounded photon information efficiencies (PIEs). However, a number of limitations of a physical system limit the practically achievable PIE. In this paper, we discuss several of these limitations and illustrate their impact on the channel. We show that, for the Poisson channel, noise does not strictly bound PIE, although there is an effective limit, as the dimensional information efficiency goes as $e^{-e^{PIE}}$ beyond a threshold PIE. Since the Holevo limit is bounded in the presence of noise, this illustrates that the Poisson approximation is invalid at large PIE for any number of noise modes. We show that a finite transmitter extinction ratio bounds the achievable PIE to a maximum that is logarithmic in the extinction ratio. We show how detector jitter limits the ability to mitigate noise in the PPM signaling framework. We illustrate a method to model detector blocking when the number of detectors is large, and illustrate mitigation of blocking with spatial spreading and filtering. Finally, we illustrate the design of a high photon efficiency system using state-of-the-art photo-detectors and taking all these effects into account.

Keywords: optical communications, quantum-limited communications, photon-counting detectors, photon information efficiency

1. INTRODUCTION

An optical communications channel may be characterized by its efficiency in utilizing available resources to transmit information. The resources of interest are the transmitted power and the bandwidth occupancy, or, more generally, the number of dimensions (temporal, spatial, or polarization) occupied by the signal. Let C denote the channel *capacity*, the maximum rate of information transmission, in bits per unit time. The power, or photon, efficiency is given by

$$c_p = \frac{C}{\bar{n}_s} \text{ (bits/photon)}$$

where $\bar{n}_s$ is the mean photon cost per unit time. Similarly, the dimensional efficiency is given by

$$c_d = \frac{C}{M} \text{ (bits/dimension)}$$

where M is the number of dimensions required to span the collection of signals that may be transmitted per unit time. The bound on achievable pairs (c_p, c_d) is given by the *Holevo* limit,

$$c_d^{\text{Hol}} = (1+\bar{n}_s)\log_2(1+\bar{n}_s) - \bar{n}_s \log_2(\bar{n}_s)$$
$$c_p^{\text{Hol}} = c_d^{\text{Hol}}/\bar{n}_s$$

The largest c_p demonstrations to date have utilized on-off-keying (OOK) with a photon-counting receiver, see, e.g., Ref. 1–5. The OOK channel may be modeled as follows. In a channel use, a slot of duration T_s seconds,

 Send correspondence to bmoision@jpl.nasa.gov. The research described in this publication was supported by the DARPA InPHo program under contract JPL 97-15402, and the JPL R&TD Program, and was carried out by the Jet Propulsion Laboratory, California Institute of Technology, under a contract with the National Aeronautics and Space Administration

either a pulse is transmitted, with probability p (transmitting a '1'), or no pulse is transmitted, with probability $(1-p)$ (transmitting a '0'). In a pulsed slot we receive a Poisson-distributed photon count with mean n_s (in a non-pulsed slot we receive no counts). The capacity of this OOK channel is given by

$$C^{\text{OOK}}(0) = h_2\left(p(1-e^{-n_s})\right) - ph_2(e^{-n_s}) \text{ (bits/slot)} \tag{1}$$

where $h_2(x) = -x\log_2 x - (1-x)\log_2(1-x)$ is the binary entropy function. The photon and dimensional efficiencies are given by

$$c_p^{\text{OOK}} = \frac{C^{\text{OOK}}(0)}{pn_s}, \qquad c_d^{\text{OOK}} = C^{\text{OOK}}(0)$$

Let

$$c_d^*(c_p^*) = \max_{(n_s,p)|c_p=c_p^*} c_d \tag{2}$$

and let $\mathcal{C}^{\text{OOK}}(0)$ denote the convex hull of the collection of points $(c_p^*, c_d^*(c_p^*))$ for the ideal, noiseless OOK channel. At large c_p^*, we have[6]

$$c_d^* \approx \frac{2}{e\ln(2)} 2^{-c_p^*} \tag{3}$$

Hence c_p can grow no faster than logarithmically in c_d.

In this paper we discuss non-ideal system components and operating conditions that bound one away from the theoretical limit given by (1), (3). The paper is organized as follows. In Section 2 we consider the impact of background or dark noise, and show that, while noise does not strictly bound c_p for the Poisson channel, it effectively bounds it, as c_d goes as $e^{-e^{c_p}}$ at large c_p. In Section 3 we show that a finite transmitter extinction ratio bounds the achievable c_p, and discuss a demonstration of a high extinction-ratio transmitter. In Section 4 we briefly discuss detector jitter and illustrate that it limits the ability to mitigate noise. In Section 5 we discuss the impact of detector blocking, methods to model it for arrays of detectors, and methods to mitigate it with spatial spreading and filtering. Finally, in Section 6 we provide an example design of a high photon efficiency free-space channel, taking into account the physical limitations discussed in prior sections, and using parameters of current state-of-the art photo-detectors.

We model the photon-counting channel as follows. In Sections 2, 3, 4 and 5, we implicitly assume a detection efficiency of one, so that each incident photon produces a photo-electron. Only in Section 6 do we explicitly take into account the detection efficiency. We assume throughout that the background noise coupling into the photo-detector is either zero, or that the number of noise modes is sufficiently large that the photo-detector output is well modeled as a Poisson point process.[7] Hence the results on the noisy channel may more properly be attributed to the intensity modulated Poisson channel. Care should be taken in applying these results generally to the photon-counting channel outside the region of zero noise, or where the Poisson approximation holds. We show, for example, that the Poisson channel efficiencies are unbounded in the presence of noise, whereas the Holevo limit is bounded, hence the Poisson approximation must break down at large photon efficiencies, regardless of the number of noise modes.

2. NOISE

The first degradation we consider is noise. Noise (non-signal) photo-electrons will be present due to incident background light or photo-detector dark noise. Let n_b be the mean noise photo-electrons per slot. Let $p_1(k), p_0(k)$ denote the probabilities of k counts in a pulsed slot and non-pulsed slot, respectively. We have

$$p_1(k) = \frac{e^{-(n_s+n_b)}(n_s+n_b)^k}{k!}$$
$$p_0(k) = \frac{e^{-n_b}(n_b)^k}{k!}$$

and the OOK channel capacity in noise is given by[8]

$$C^{\text{OOK}}(n_b) = -pE\left(\log_2\left(p + (1-p)L^{-1}(Y_1)\right)\right) - (1-p)E\left(\log_2\left(1 - p + pL(Y_0)\right)\right) \tag{4}$$

where $L(y) = p_1(y)/p_0(y)$, $E(\cdot)$ denotes the expected value, $Y_1 \sim p_1$ and $Y_0 \sim p_0$. The photon and dimensional efficiencies of OOK in noise are $c_p^{\text{OOK}} = C^{\text{OOK}}(n_b)/pn_s$ and $c_d^{\text{OOK}} = C^{\text{OOK}}(n_b)$. Let $\mathcal{C}^{\text{OOK}}(n_b)$ denote the convex hull of achievable pairs (c_p^*, c_d^*) defined by (2) for the noisy channel. Figure 1 illustrates $\mathcal{C}^{\text{OOK}}(n_b)$, evaluated numerically for $n_b \in \{10^{-2}, 10^{-3}, 10^{-4}, 10^{-5}, 10^{-6}, 10^{-7}\}$.

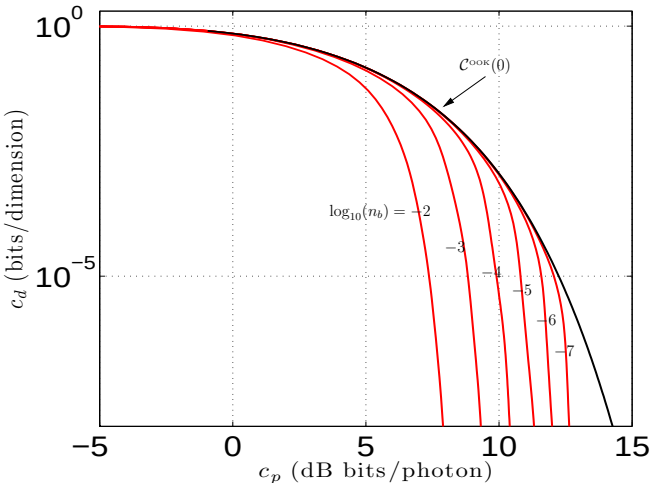

Figure 1. Achievable PIE, DIE of photon-counting OOK in the presence of noise. $\mathcal{C}^{\text{OOK}}(n_b)$, $n_b > 0$, labeled with $\log_{10}(n_b)$.

2.1 Poisson channel c_p is unbounded in the presence of noise

Let $M = 1/p$. For M a power of two, the OOK capacity with duty cycle p is bounded by the PPM capacity with order M:[8]

$$C^{\text{OOK}}(n_b) \geq C^{\text{PPM}}(n_b) = \frac{1}{M}\left(D(p_1||p_0) - E_Y \log_2 \frac{1}{M}\sum_{j=1}^{M} L(Y_j)\right) \text{ (bits/slot)} \tag{5}$$

where $D(u||v)$ is the Kullback-Leibler distance between distributions u and v, $Y = (Y_1, \ldots, Y_M)$ is a vector with $Y_i, Y_j, i \neq j$, independent, $Y_1 \sim p_1$ and $Y_j \sim p_0$ for $j \neq 1$. From Jensen's inequality, this may be further lower bounded as

$$C^{\text{PPM}}(n_b) \geq \frac{1}{M}\left(D(p_1||p_0) - \log_2 \frac{1}{M}\sum_{j=1}^{M} E(L(Y_j))\right)$$

Now

$$E(L(Y_j)) = \begin{cases} \exp(n_s^2/n_b) & , j = 1 \\ 1 & , j \neq 1 \end{cases}$$

and

$$D(p_1||p_0) = (n_s + n_b)\log_2(1 + n_s/n_b) - n_s/\ln(2)$$

Hence

$$c_p^{\text{OOK}}(n_b) \geq (1 + n_b/n_s)\log_2(1 + n_s/n_b) - 1/\ln(2) + \frac{1}{n_s}\log_2\left(\frac{M}{M - 1 + e^{n_s^2/n_b}}\right)$$

The first term grows as $\log_2(n_s/n_b)$ for sufficiently large n_s. By choosing $M = e^{n_s^2/n_b} - 1$, the final term goes to zero for large n_s. Hence c_p can be made arbitrarily large for any n_b. The single-mode Holevo capacity in background noise is given by[9]

$$C^{\mathrm{Hol}}(n_b) = g(\bar{n}_s + n_b) - g(n_b)$$

where $g(x) = (1+x)\log_2(1+x) - x\log_2(x)$, and $\bar{n}_s$ is the mean photon number. For $\bar{n}_s \ll n_b$, we have

$$C^{\mathrm{Hol}}(n_b) = \bar{n}_s \log_2(1 + 1/n_b) + o(\bar{n}_s)$$

Let $c_p^{\mathrm{Hol}}(n_b) = C^{\mathrm{Hol}}(n_b)/\bar{n}_s$, the Holevo photon-information-efficiency. This increases with $1/\bar{n}_s$ at large $c_p^{\mathrm{Hol}}(n_b)$ to the limit

$$c_p^{\mathrm{Hol}}(n_b) \xrightarrow[\bar{n}_s \to 0]{} \log_2(1 + 1/n_b)$$

Hence $c_p^{\mathrm{Hol}}(n_b)$ is bounded. Since the Holevo limit bounds any intensity-modulated photon-counting receiver, the Poisson approximation must break down at large c_p, for any number of noise modes.

2.2 Poisson channel c_p is effectively bounded in the presence of noise

For $n_b > 0$, the noisy PPM capacity may be upper bounded by[10]

$$C^{\mathrm{PPM}}(n_b) < \frac{1}{M}\left(D(p_1||p_0) - D(p_{\bar{1}}||p_{\bar{0}})\right) \tag{6}$$

where

$$p_{\bar{1}}(k) = \frac{e^{-(n_s + Mn_b)}(n_s + Mn_b)^k}{k!}$$
$$p_{\bar{0}}(k) = \frac{e^{-Mn_b}(Mn_b)^k}{k!}$$

The noiseless PPM capacity is given by $C^{\mathrm{PPM}}(0) = \log_2(M)(1 - e^{-n_s})/M$. Since the divergence is non-negative, and the capacity is decreasing with n_b, we have the bound

$$C^{\mathrm{PPM}}(n_b) \le \frac{1}{M}\min\{D(p_1||p_0), \log_2(M)(1 - e^{-n_s})\}$$

Hence

$$c_p^{\mathrm{PPM}}(n_b) \le \min\left\{D(p_1||p_0)/n_s, \log_2(M)(1 - e^{-n_s})/n_s\right\} \tag{7}$$
$$c_d^{\mathrm{PPM}}(n_b) \le \min\left\{D(p_1||p_0)/M, \log_2(M)(1 - e^{-n_s})/M\right\} \tag{8}$$

Consider (7). $D(p_1||p_0)/n_s$ is increasing in n_s and is zero at $n_s = 0$ whereas $\log_2(M)(1 - e^{-n_s})/n_s$ in decreasing in n_s and goes to $\log_2 M$ as $n_s \to 0$. Hence the bound is maximized over n_s for fixed M when the terms are equal, that is,

$$\begin{aligned}\tilde{c}_p &\stackrel{\mathrm{def}}{=} \max_{n_s} \min\left\{D(p_1||p_0)/n_s, \log_2(M)(1 - e^{-n_s})/n_s\right\} \\ &= \frac{\log_2(M^*)(1 - e^{-n_s^*})}{n_s^*}\end{aligned} \tag{9}$$

where (M^*, n_s^*) satisfy

$$(n_s^* + n_b)\ln(1 + n_s^*/n_b) - n_s^* = \ln(M^*)(1 - e^{-n_s^*}). \tag{10}$$

Consider (8), and let

$$\tilde{c}_d \stackrel{\text{def}}{=} \max_{n_s} \min \left\{ D(p_1||p_0)/M, \log_2(M)(1-e^{-n_s})/M \right\}$$

We'll show that $\tilde{c}_d = \tilde{c}_p n_s^*/M^*$. Note that

$$\frac{\partial}{\partial n_s}\left(\log_2(M)(1-e^{-n_s})\right) = e^{-n_s}\log_2(M) \xrightarrow[n_s\to 0]{} \log_2(M)$$
$$\frac{\partial}{\partial n_s} D(p_1||p_0) = \log_2(1+n_s/n_b) \xrightarrow[n_s\to 0]{} 0$$

Since the slope of $D(p_1||p_0)$ is increasing in n_s, is zero at zero, whereas the slope of $\log_2(M)(1-e^{-n_s})$ is decreasing in n_s, and is positive at zero, and both functions go to zero as $n_s \to 0$, it follows similarly that $\tilde{c}_d$ is achieved when the terms in (9) are equal, that is, that

$$\tilde{c}_d = \tilde{c}_p n_s^*/M^*$$

Let $\mathcal{C}^{\text{PPM}}(n_b)$ denote the collection of dominating pairs $(c_p^{\text{PPM}}, c_d^{\text{PPM}})$ defined by (2), with $P = 1/M$. The pairs $(\tilde{c}_p, \tilde{c}_d)$, parameterized by (n_s^*, M^*) bound $\mathcal{C}^{\text{PPM}}(n_b)$. We are interested in the behavior of $\mathcal{C}^{\text{PPM}}(n_b)$ for large c_p. One can show $\tilde{c}_p$ increases without bound in n_s^*. Hence the large $\tilde{c}_p$ behavior corresponds to large n_s^*. From (9), we have

$$M^* = \exp\left(\frac{\tilde{c}_p \ln(2) n_s^*}{1-e^{-n_s^*}}\right)$$

and, from (10), at large n_s^*/n_b we have

$$\tilde{c}_p \approx \log_2(n_s^*/n_b) - 1/\ln(2)$$
$$n_s^* \approx n_b \exp(1+\tilde{c}_p \ln(2))$$

Hence,

$$\tilde{c}_d \approx n_b \tilde{c}_p \exp(\tilde{c}_p \ln(2)+1) \exp\left(\frac{-n_b \tilde{c}_p \ln(2) \exp(\tilde{c}_p \ln(2)+1)}{1-\exp(-n_b \exp(\tilde{c}_p \ln(2)+1))}\right) \tag{11}$$

and, although $\tilde{c}_p$ is not strictly bounded, $\tilde{c}_d$ falls off as $e^{-e^{\tilde{c}_p}}$ at large $\tilde{c}_p$, so that, for practical purposes, we may think of $\tilde{c}_p$ as bounded due to noise. Since the large c_p asymptotes of PPM and OOK agree, (11) approximates $\mathcal{C}^{\text{OOK}}(n_b)$ at large c_p as well.

3. EXTINCTION RATIO

Let P_1 denote the average power emitted from the laser transmitter in the on state. Certain laser transmitters emit some power $P_0 = P_1/\alpha$ in the off state, where α is referred to as the *extinction ratio*. We show here that a finite extinction ratio bounds the achievable c_p.

Let l_p be the peak received signal photon rate and l_d the received photon rate from all non-signal sources, assumed constant. Let l_s denote the mean signal photon rate, and p the duty cycle. Some of the average power bleeds into the 'off' positions, so the relationship between the average and peak rates is

$$l_p = \frac{\alpha l_s}{p(\alpha-1)+1}$$

This channel is equivalent to a channel with peak signal rate $l_p' = l_p(1-1/\alpha)$ received in noise with rate $l_n' = l_d + l_p/\alpha$. In order to obtain a bound on performance attributed only to the extinction ratio, suppose the

only photons received in the 'off' state are due to non-extincted signal photons, i.e., that $l_d = 0$. The equivalent channel then has mean signal and noise rates

$$l_s' = \frac{\alpha - 1}{\alpha - 1 + 1/p} l_s$$
$$l_n' = \frac{1/p}{\alpha - 1 + 1/p} l_s$$

Let

$$\psi = \frac{l_s'}{l_n'} = p(\alpha - 1)$$

the signal-to-noise ratio.

We consider two notions of the photon-information-efficiency for this channel. In the first, in computing the photon cost we count all received signal photons (with rate l_s), whether they fall in the signal slot or not. In the second, in computing the photon cost, we count only those photons that fall in the signal slot–those that are *effectively* received as signal photons (with rate l_s'). Letting C^{OOK} denote the information rate, in bits/s, and putting rates in units of photons/s, define

$$c_{p,0} = \frac{C^{\text{OOK}}}{l_s} \text{ (bits/signal photon)}$$
$$c_{p,1} = \frac{C^{\text{OOK}}}{l_s'} \text{ (bits/effective signal photon)}$$

For $p < 1/e$ the information rate (the same for either units) is bounded by[10]

$$\begin{aligned} C^{\text{OOK}} \le \tilde{C} &\stackrel{\text{def}}{=} l_s' \left(\left(1 + \frac{p}{\psi}\right) \log_2(1 + \psi/p) - \left(1 + \frac{1}{\psi}\right) \log_2(1 + \psi) \right) \text{ bits/s} \\ &= l_s \left(\frac{\alpha p}{p(\alpha - 1) + 1} \log_2(\alpha) - \log_2(1 + p(\alpha - 1)) \right) \text{ bits/s} \end{aligned} \tag{12}$$

We'll consider the two cases separately.

3.1 Bits/Signal Photon

When all transmitted photons are included in the photon efficiency, we have

$$\begin{aligned} c_{p,0} \le \tilde{c}_{p,0} &\stackrel{\text{def}}{=} \tilde{C}/l_s \\ &= \left(\frac{\alpha}{\alpha - 1 + 1/p} \log_2(\alpha) - \log_2(1 + p(\alpha - 1)) \right) \end{aligned}$$

Since

$$\frac{d\tilde{c}_{p,0}}{dp} = \left(\frac{\alpha \ln(\alpha) - (\alpha - 1) - p(\alpha - 1)^2}{(p(\alpha - 1) + 1)^2} \right) \frac{1}{\ln(2)}$$

there is an optimum duty cycle,

$$p^* = \frac{\alpha \ln(\alpha) - (\alpha - 1)}{(\alpha - 1)^2}$$

with resulting maximum

$$\max_p \tilde{c}_{p,0} = \left(\frac{\alpha \ln \alpha}{\alpha - 1} - \ln \left(\frac{\alpha \ln \alpha}{\alpha - 1} \right) - 1 \right) \frac{1}{\ln(2)}$$

Hence $c_{p,0}$ is bounded.

3.2 Bits/Effective Signal Photon

When only photons that effectively act as signal photons are included in the photon efficiency, we have

$$\begin{aligned} c_{p,1} \le \tilde{c}_{p,1} &\stackrel{\text{def}}{=} \tilde{C}/l'_s \\ &= \left(\frac{\alpha}{\alpha - 1} \log_2(\alpha) - \left(1 + \frac{1}{p(\alpha - 1)} \right) \log_2(1 + p(\alpha - 1)) \right) \end{aligned}$$

and, since

$$\frac{d\tilde{c}_{p,1}(p)}{dp} = -\left(\frac{1}{p} + \frac{\ln(1 + p(\alpha - 1))}{(\alpha - 1)p^2} \right) \frac{1}{\ln(2)} \le 0$$

we see that $c_{p,1}$ is increasing with $1/p$. It increases to the limit

$$\begin{aligned} \lim_{p \to 0} \tilde{c}_{p,1} &= \frac{\alpha}{\alpha - 1} \log_2(\alpha) - 1/\ln(2) \\ &\approx \log_2(\alpha) - 1/\ln(2) \end{aligned}$$

Hence with either accounting of the photon cost, the bits/photon is bounded with a finite extinction ratio.

3.3 High Extinction Ratio Demonstration

We've shown that large extinction ratios are required to achieve large c_p. For example, to achieve $c_{p,1} = 10$ bits/photon would require an extinction ratio greater than 34 dB. That assumes all other system components are ideal and that one achieves the system capacity. If we factor in code inefficiency and any other practical losses, the required extinction ratio becomes much larger.

We demonstrated a high extinction ratio modulator based upon a cascade of a semiconductor optical amplifier (SOA) with conventional Mach-Zender electrooptic modulator (EOM). The SOA is operated to provide approximately 40 dB of isolation in the "off" state, and 10 dB of gain in the "on" state, followed by approximately 25 dB of isolation in the "off" state from the EOM. Unlike cascaded EOM's, the extinction ratios from the SOA EOM cascade directly add.

The high extinction ratio of the SOA EOM cascade was validated by making time-resolved extinction ratio measurements using a multi-channel analyzer with 1 ns bins. A block diagram of the experimental setup is illustrated in Figure 2. The detector for this measurement was a NbTiN superconducting nanowire detector fabricated at JPL's Microdevices Laboratory and operated at a bias current that provided approximately 40% detection efficiency with a 0.1 Hz dark rate. Figure 3 illustrates histograms collected over 10^8 frames: one with only dark counts, one with pulsed frames, and a closer look at the pulsed region of the pulsed frame. The peaks 30 dB and more down from the main peak are the results of electrical reflections in the modulator drive electronics. Analysis based on this data confirms a greater than 76 dB extinction ratio between the "on" and "off" modulator states.

4. JITTER

With an ideal photo-detector, the intensity function of photo-electrons is proportional to the energy of the incident field. Hence an ideal signal pulse that is uniform over the duration of a slot would give rise to photo-electrons distributed uniformly over the slot. However, in non-ideal photo-detectors, there is a random delay between the arrival of a photon on the photo-sensitive surface and the generation of a corresponding photo-electron or current pulse. We refer to this random delay as *detector jitter*.

In the context of signaling with PPM, if detector jitter yields non-orthogonal PPM symbols, it produces a loss relative to the non-jittered case. The capacity loss was treated in Ref. 11, 12, and an approximation to the loss in Ref. 13. Here we restate the approximation.

Let the jitter be Gaussian distributed with standard deviation σ. Suppose we are signaling with order M PPM, error-control-code rate R, slot-width T_s, and that the signal is received in noise with rate n_b photons/slot.

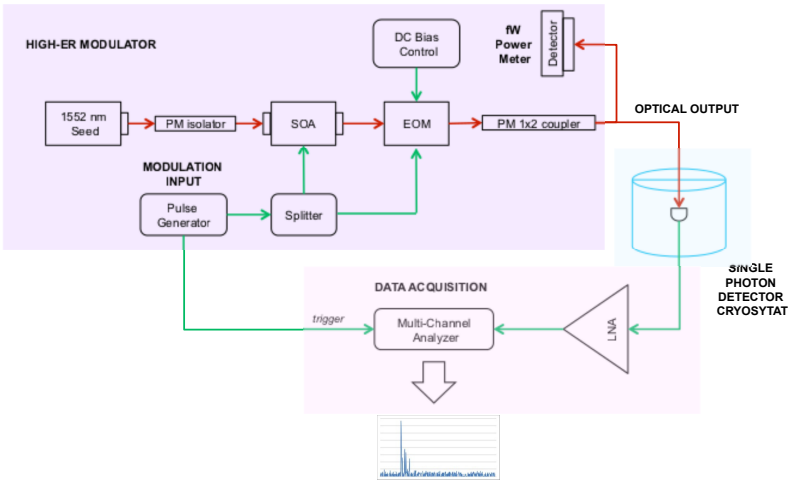

Figure 2. Experimental setup demonstrating a high extinction ratio modulator

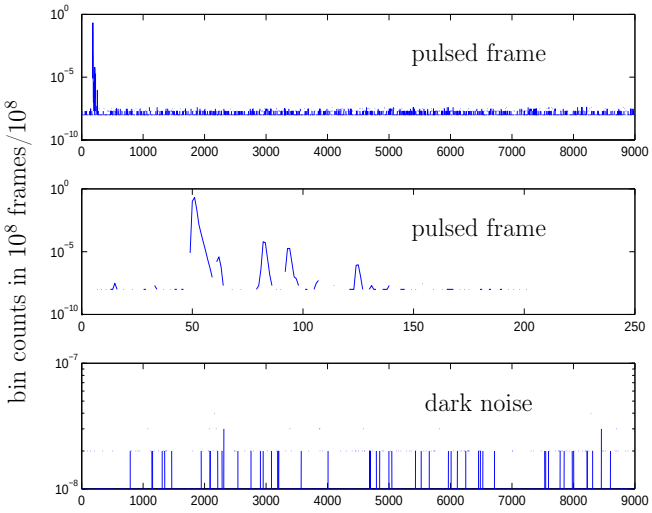

Figure 3. Photon counts from a demonstration of a 76 dB extinction ratio modulator

The exact loss is a function of the quintuple (M, R, T_s, σ, n_b). Let l_s denote the average signal photon rate, in photons/s, required to achieve a capacity equal to the target data rate in the absence of jitter and l_s' the corresponding rate required in the presence of jitter. It was shown in Ref. 13 that the signal power loss may be approximated as

$$\left(\frac{l_s}{l_s'}\right) \approx 5.0\Psi^2 + 2.0\Psi + 1$$

where

$$\Psi = \left(\frac{\sigma}{T_s}\right) \frac{(1 + \tanh(R - 1/2))}{(1.25)^{\log_2(M)}}$$

For $\Psi = 0.1$, the loss is ≈ 1 dB. For a device with a specified σ, losses due to jitter may be mitigated by increasing

T_s or increasing M. Both decrease the data rate. Moreover, increasing T_s increases n_b for fixed background or dark rate (in counts/s). Hence there is an optimum slotwidth that minimizes losses due to jitter and noise.

5. BLOCKING

After the production of a photo-electron, a photo-detector is incapable of producing another photo-electron for some τ seconds, a phenomenon referred to as blocking. Blocking results in attenuation of the mean detected photo-electron rates and alters the statistics of the observed point process. The degradation for a single detector was treated in Ref. 14. In practice, arrays of detectors are commonly used to increase the active collecting area and facilitate tracking algorithms and spatial filtering. A collection of the detector outputs are summed to form an aggregate point process. Although weighted combining is ideal, on-off combining suffers only a small loss,[15] and does not require estimation of the individual signal and noise rates. If the number of detectors is large, the aggregate process may be modeled as Poisson.[16] In this case, the loss due to blocking may be accurately modeled as an attenuation of the rate functions. In this section, we treat that case, and discuss mitigating blocking by spreading the signal spatially and using a spatial filter.

5.1 Rate Attenuation

The rate attenuation may be modeled via a Markov chain analysis, as described in Ref. 14. When $\tau \geq T_s$, the analysis may be simplified, as we describe here. For notational convenience we assume T_s divides τ. We also assume that slots are modulated independently (that is, as generalized OOK rather than PPM). This is a good approximation to PPM for moderate blocking.[17] Let $L = \tau/T_s$, and model the detector state with the $L+1$ state Markov chain illustrated in Figure 4. Let l_s denote the mean incident signal photon rate and l_n denote the mean background photon rate. The detector is unblocked in state 0, and otherwise blocked. The transition probability to remain in the unblocked state is

$$q_0 = (1-p)e^{-l_n T_s} + pe^{-T_s(l_s/p+l_n)} \tag{13}$$

and the steady-state probability of being in the unblocked state is

$$\mu_0 = \frac{1}{1+L(1-q_0)}$$

Since $\tau \geq T_s$, the mean detected photons in an un-pulsed slot, denoted n_b, is the probability of a count in that slot

$$\begin{aligned} n_b = P(\text{count}|\text{slot is not pulsed}) &= P(\text{unblocked, detected arrival}|\text{slot is not pulsed}) \\ &= P(\text{unblocked})P(\text{detected arrival}|\text{slot is not pulsed}) \\ &= \mu_0(1-e^{-l_n T_s}) \end{aligned} \tag{14}$$

Similarly, the mean detected photons in a pulsed slot, $n_s + n_b$, is given by

$$n_s + n_b = P(\text{count}|\text{slot is pulsed}) = \mu_0(1-e^{-T_s(l_s/p+l_n)}) \tag{15}$$

where n_s denotes the portion of the mean count attributed to signal photo-electrons.

Blocking may be mitigated by decreasing the peak rate per detector. This can be accomplished by making the signal more diffuse in either space or time. However, spreading the signal also forces the receiver to integrate more noise when capturing the signal. Hence there is an optimum operating point that trades off reducing blocking for increasing noise.

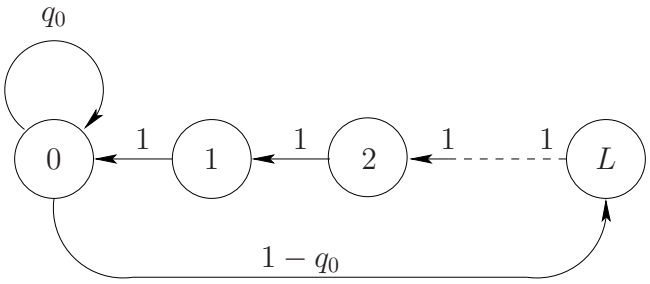

Figure 4. Markov model of detector state

5.2 Spatial Filtering

Suppose the signal is incident on an array of detectors. Let $(n_{s,i}, n_{b,i})$ denote the mean signal and noise photons per slot at the output (the post-blocking rate) of the ith detector. The receiver sums the outputs of a collection S of the detectors, so that, under the Poisson approximation, the signal and noise counts per slot are Poisson random variables, with means

$$n_s = \sum_{i \in S} n_{s,i}$$
$$n_b = \sum_{i \in S} n_{b,i}$$

The choice of S implements a spatial filter, discarding all but the most informative outputs. We consider two methods to select S. Each is a greedy search algorithm, one based on the flux rate of each detector, the other on the distance from the center of the point spread function. We first describe the rate-based-selection. Place the signal contributions in increasing order $n_{s,1} \geq n_{s,2} \geq \cdots$. Let

$$n_s(K) = \sum_{i=1}^{K} n_{s,i}$$
$$n_b(K) = \sum_{i=1}^{K} n_{b,i}$$

and let $C(K)$ be the capacity of channel with rates $(n_s(K), n_b(K))$. We conjecture that choosing K to maximize $C(K)$ maximizes the capacity.

To implement the rate-selection search requires one to measure the signal and noise rates at the output of each detector. This may be problematic in practice. We also consider the following distance-selection search. Similar to the rate-selection search, the detectors are placed in order of increasing distance from center of the point-spread-function, and the collection of the K closest detectors whose sum has the largest maximum capacity is chosen. With a radially symmetric pattern, such as in the diffraction-limited case, the two searches are essentially identical. Testing a fixed collection of masks corresponding to a discrete set of distances, e.g., a 2×2 square, a 3×3 cross, a 3×3 square, etc., is near optimum in these cases, and represents a practical solution to a spatial filter.

6. EXAMPLE: A HIGH PHOTON-EFFICIENCY FREE-SPACE OPTICAL LINK

In this section, we combine the prior results, using parameters that reflect current state-of-the-art photon-detector technology, to design a high photon-efficiency free-space optical link. Suppose we have an optical terminal receiving a free-space intensity-modulated PPM signal in the far-field, transmitted with an extinction ratio of 75 dB, and slot-widths of $T_s = 1.0$ ns. The receive aperture has a diameter of $D = 1.0$ m, and the focal plane is populated with an array of photon-counting photo detectors of width 2δ (we model these as square pixels, perfectly tiling the focal plane). The photo-detectors have a detection efficiency of η, a dead time of

τ seconds, a jitter of σ seconds, and a dark rate proportional to their active area of l_d. We assume noise is dominated by dark counts and non-extincted signal photons, and set background noise to zero.

We consider three candidate photon counters, with parameters listed in Table 1*. These represent current leading candidates for high photon-efficiency photon-counting communication links. In all numerical results, we assume the point-spread-function (PSF) is a diffraction limited Airy pattern, and that a pointing and tracking system has centered the spot at the intersection of four detectors†. In all numerical results, we select, for each operating point, an optimum PPM order M, and a collection of detectors from the greedy-rate-search ‡.

Device	Detection Efficiency η	Dark Rate l_d $(e/s/\mathrm{mm}^2)$	Diameter 2δ (μm)	Dead-Time $\tau(ns)$	Jitter $\sigma(ps)$
Si GM-APD	0.40	10^6	15.0	50	240
InGaAs(P) GM-APD	0.55	10^8	15.0	10^4	300
Nb(Ti)N Nanowire	0.5	10^2	5.0	20	30

Table 1. Representative parameters for photon-counting devices

We are free to choose the focal length F to spread the signal spatially. A smaller focal length produces a smaller spot, with a higher signal intensity in the focal plane. This leads to larger losses due to blocking, but, since a smaller integrated area is required, a smaller dark noise contribution. In the limit of no blocking ($\tau = 0$), the performance improves with decreasing F (up to the limits of the quantization of the focal plane due to the finite pixel area), as one filters out dark noise. Conversely, in the limit of no dark noise ($l_d = 0$), the performance improves with increasing F, as the signal and background noise become more diffuse, and blocking losses become negligible. In the general case there is an optimum focal length.

In order to illustrate the range of achievable photon and dimensional efficiencies, we varied the incident signal radiance, and determined the optimum F-number, optimum PPM order, and subsequent capacity at each point. Jitter is modeled as in Ref. 12 (we do not use the approximation from Section 4). Blocking is modeled as a rate attenuation, as described in Section 5. The resulting (c_p, c_d) pairs are illustrated in Figure 5. Also illustrated is the (noiseless) Holevo bound and the ideal OOK capacity ($\eta = 1.0, \tau = 0, l_d = 0$), which bounds the performance of the practical detectors. This illustrates the degradation due to a finite detection efficiency, dark noise, and blocking for the three detectors. In order to isolate the degradation due only to blocking, jitter, extinction ratio, and dark noise, Figure 6 illustrates (c_p/η, c_d), factoring out the loss in photon efficiency due to the detection efficiency. Here we see that the sub-unity detection efficiency is the primary impediment for the Si GM and NbN nanowire detectors.

ACKNOWLEDGMENTS

We would like to thank William Wu for discussions on bounding the information efficiencies in the presence of noise.

REFERENCES

[1] Lesh, J., Katz, J., Tan, H., and Zwilliinger, D., "2.5-bit/detected photon demonstration program: Description, analysis, and phase I results," *TDA Progress Report* **42–66**, 115–132 (September 1981).

[2] Robinson, B., Caplan, D., Stevens, M., Barron, R., Dauler, E., and Hamilton, S., "1.5-photons/bit photon-counting optical communications using geiger-mode avalanche photodiodes," in [*LEOS Summer Topical Meetings, 2005 Digest of the*], 41–42 (July 2005).

*William Farr, "VIS/NIR Optical Communications Single Photon Detector Technologies Characterized in JPL's Detector Calibration Facility"

†We also evaluated randomly dithering the PSF position, which has little impact on the average performance.

‡Greedy-distance-searches yielded only small losses relative to this.

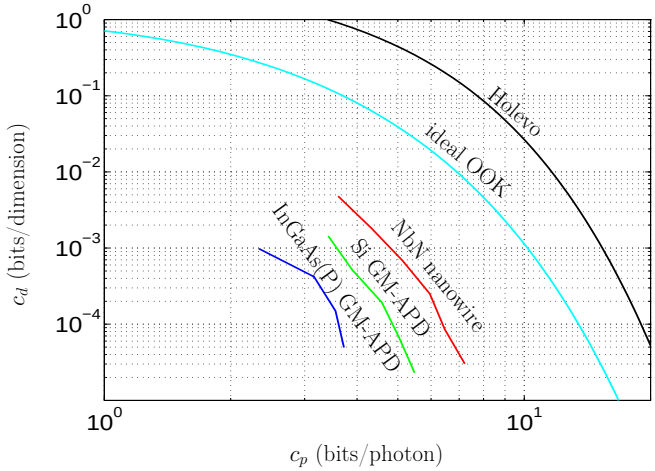

Figure 5. Achievable (dimensional efficiency, photon efficiency) pairs for the three candidate detectors, with comparison to the ideal OOK limit, $\mathcal{C}^{\text{OOK}}(0)$, and the Holevo bound.

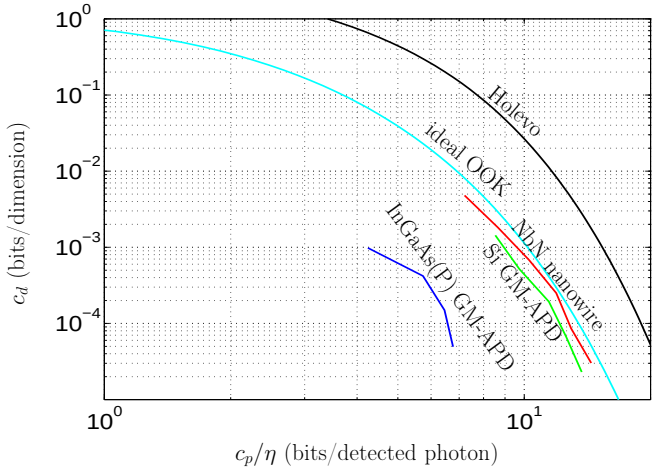

Figure 6. Achievable (dimensional efficiency, photon efficiency) pairs for the three candidate detectors, with photon efficiency factoring out the degradation due to non-unity detection efficiency η, with comparison to the ideal OOK limit $\mathcal{C}^{\text{OOK}}(0)$, and the Holevo bound.

[3] Dauler, E., Robinson, B., Kerman, A., Anant, V., Barron, R., Berggre, K., Caplan, D., Carney, J., Hamilton, S., adn M.L. Stevens, K. R., and Yang, J., "1.25-Gbit/s photon-counting optical communications using a two-element superconducting nanowire single photon detector," in [*Proceedings of the SPIE*], **6372** (October 2006).

[4] Robinson, B. S., Kerman, A. J., Dauler, E. A., Boroson, D. M., Hamilton, S. A., Yang, J. K. W., Anant, V., and Berggren, K. K., "Demonstration of gigabit-per-second and higher data rates at extremely high efficiency using superconducting nanowire single photon detectors," in [*Proceedings of the SPIE*], **6709** (Aug. 2007).

[5] Birnbaum, K., Farr, W., Gin, J., Moision, B., Quirk, K., and Wright, M., "Demonstration of a high-efficiency free-space optical communications link," in [*Proceedings of the SPIE*], **7199** (January 2009).

[6] Erkmen, B. I., Moision, B. E., Dolinar, S. J., Birnbaum, K. M., and Divsalar, D., "On approaching the ultimate limits of communication using a photon-counting detector," in [*Proceedings of the SPIE*], (January 2012).

[7] Gagliardi, R. M. and Karp, S., [*Optical Communications*], John Wiley & Sons, New York, 2 ed. (1995).

[8] Moision, B. and Hamkins, J., "Deep-space optical communications downlink budget: Modulation and Coding," *IPN Progress Report* **42-154** (Aug. 2003).

[9] Erkmen, B. I., Moision, B. E., and Birnbaum, K. M., "The classical capacity of single-mode free-space optical communications: A review," *IPN Progress Report* **42-179** (November 2009).

[10] Wyner, A. D., "Capacity and error exponent for the direct detection photon channel–Part I," *IEEE Transactions on Information Theory* **34**, 1449–1461 (Nov. 1988).

[11] Kachelmyer, A. and Boroson, D. M., "Efficiency penalty of photon-counting with timing jitter," in [*Proceedings of the SPIE*], **6709** (Aug. 2007).

[12] Moision, B. and Farr, W., "Communication limits due to photon detector jitter," *IEEE Photonics Technology Letters* **20**, 715–717 (May 2008).

[13] Moision, B., Shambayati, S., and Wu, J., "An optical communications link design tool for long-term mission planning for deep-space missions," in [*IEEE Aerospace Conference*], (March 2012).

[14] Moision, B. and Piazzolla, S., "Blocking losses on an optical communications link," in [*Space Optical Systems and Applications (ICSOS), 2011 International Conference on*], 368 –377 (May 2011).

[15] Vilnrotter, V. A. and Srinivasan, M., "Adaptive detector arrays for optical communications receivers," *IEEE Transactions on Communications* **50**, 1091–1097 (July 2002).

[16] Snyder, D. L., [*Random Point Processes*], Wiley (1975).

[17] Moision, B., Srinivasan, M., and Hamkins, J., "The blocking probability of geiger-mode avalanche photodiodes," in [*Proceedings of the SPIE*], Huang, B., Heymann, R. W., and Wang, C. C., eds., *Satellite Data Compression, Communications, and Archiving* **5889** (2005).